

PAPER • OPEN ACCESS

Photoelectric properties of heterostructures based on InAsSb_x solid solutions ($0.3 < x < 0.35$)

To cite this article: R. E. Kunkov *et al* 2020 *J. Phys.: Conf. Ser.* **1695** 012077

View the [article online](#) for updates and enhancements.



IOP | ebooks™

Bringing together innovative digital publishing with leading authors from the global scientific community.

Start exploring the collection—download the first chapter of every title for free.

Photoelectric properties of heterostructures based on InAsSb_x solid solutions (0.3 < x < 0.35).

R.E. Kunkov, A.A. Klimov, N.M. Lebedeva¹, T.C. Lukhmyrina¹, B.A. Matveev¹, M.A. Remennyi^{1,2}

¹IR Optoelectronics Laboratory, Ioffe Institute RAS, Saint Petersburg 194021, Russia

² LLC "IoffeLED", Saint Petersburg 194021, Russia

Abstract. The results of a study of multilayer p-n heterostructures based on InAsSb_x solid solution (0.3 < x < 0.35), with a long-wavelength photosensitivity boundary of $\lambda_{0.1} \approx 9.5 \mu\text{m}$ at room temperature are presented. The current-voltage and spectral characteristics of photosensitivity and electroluminescence were analyzed in the temperature range 80 ÷ 300 K. It is shown that the photoelectric properties are determined by the diffusion mechanism of current flow, and experimental samples of photodetectors are characterized by a quantum efficiency of $S_i \geq 1 \text{ A/W}$.

1. Introduction

InAsSb solid solutions are used to create photodetectors based on structures with homo and hetero p-n junctions, barrier structures with bulk layers and superlattices, photosensitive in the MWIR spectral range, operating in a wide temperature range [1]. Such photodetectors are used in gas analysis instruments, low-temperature high-speed pyrometers and thermal imaging systems.

The use of InAsSb_x solid solution with the composition region $x \geq 0.3$ opens up the possibility of using the already developed technological approaches for creating photodiode photodetectors operating in the long-wavelength region of the spectrum $\lambda = 8 \div 14 \mu\text{m}$ [2]. In this paper, we study the photoelectric properties of p-n heterostructures with the photosensitive InAsSb_x region with the composition range $0.3 < x < 0.35$ and long-wavelength photosensitivity boundary $\lambda_{0.1} \approx 9.5 \mu\text{m}$ at room temperature.

2. Experimental results

Epitaxial structures were obtained by LPE on InAs (100) substrates. A description of the photosensitive heterostructure, including the order, thickness, purpose, element content, impurity concentration and band gap for each layer is shown in Figure 1 and Table 1.



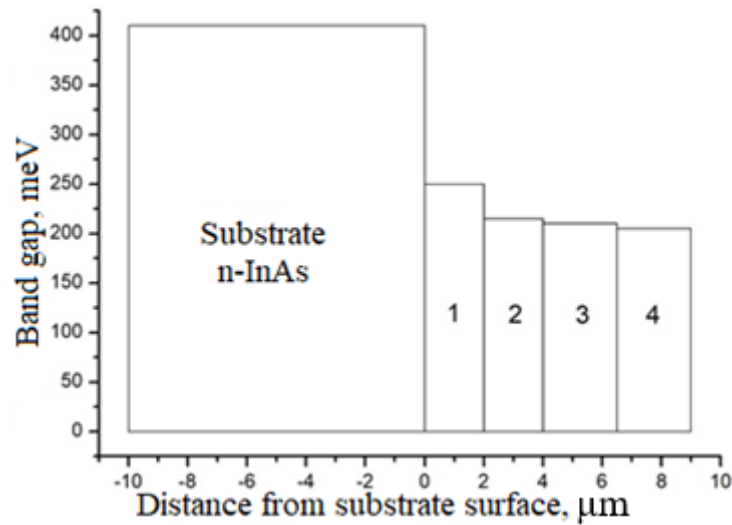


Figure 1. Sketch of the photosensitive structure (order of arrangement and characteristics of epitaxial layers).

Table 1. Description of epitaxial layers.

Layer number	Layer function	Layer composition	$\Delta a/a_{InAs}$, %	Element contents	Thickness, μm	Band gap (77 K), meV	Dopant (cm^{-3})
1	Buffer region	InAsSb _x	1.8	X = 0.25÷0.26	2.0÷2.2	250-255	-
2	Wide gap region	InAsSb _x	2.3	X = 0.34÷0.35	2.0÷2.2	210-215	-
3	Photosensitive region	InAsSb _x	2.5	X = 0.36÷0.37	2.0÷2.5	205-210	Zn, $p=(2\div5)\times E16\ cm^{-3}$
4	Photosensitive region, contact layer	InAsSb _x	2.5	X = 0.37	2.0÷2.5	205	Zn, $p=(1\div2)\times E18\ cm^{-3}$

Using multi-stage photolithography and plasma-chemical etching, we fabricated “flip-chip” samples with a photosensitive region $D = 40, 90, 180,$ and $270\ \mu m$, are shown in Figure 2. The samples were mounted on Si submount and coupled with Ge immersion lenses with a diameter of 3.5 mm. The study of electroluminescence and photoelectric characteristics was carried out in the temperature range 77-350 K using pumped cryostat, VERTEX 70v Fourier spectrometer, HgCdTe (77 K) photodetector, Keithley SourceMeter 6430 source meter and LCR E4980A precision meter.

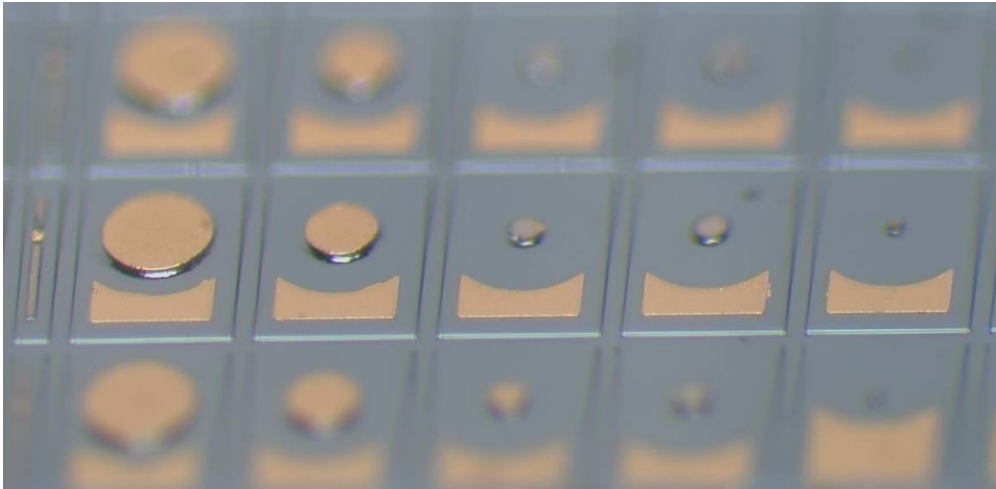


Figure 2. Photo of the surface of an epitaxial structure with mesas of single-element photodetectors with a diameter of 40, 90, 180, 260 μm .

In Figure 3 (a) shows the current-voltage characteristics of the photodetector with the size of the electrically active region $D = 180 \mu\text{m}$ in the temperature range 200-300 K.

In Figure 3 (b) shows the temperature dependences of the dark current obtained from the data in Figure 3 (a) plotted in the coordinates of the reciprocal temperature. As can be seen from the graph, the dependence has an exponential character $J_{\text{sat}} \sim 1 / \exp(E_a / kT)$ with an exponent of about $E_a = 200 \text{ meV}$, which approximately corresponds to the value of the band gap of the photosensitive region during cryogenic cooling and can be determined from the long-wavelength edge of the photosensitivity $\lambda_{0.5}$. The approximation of the dependence with an exponent corresponding to the value of E_g also indicates the diffusion mechanism of current flow in the entire temperature range of $200 \div 300 \text{ K}$.

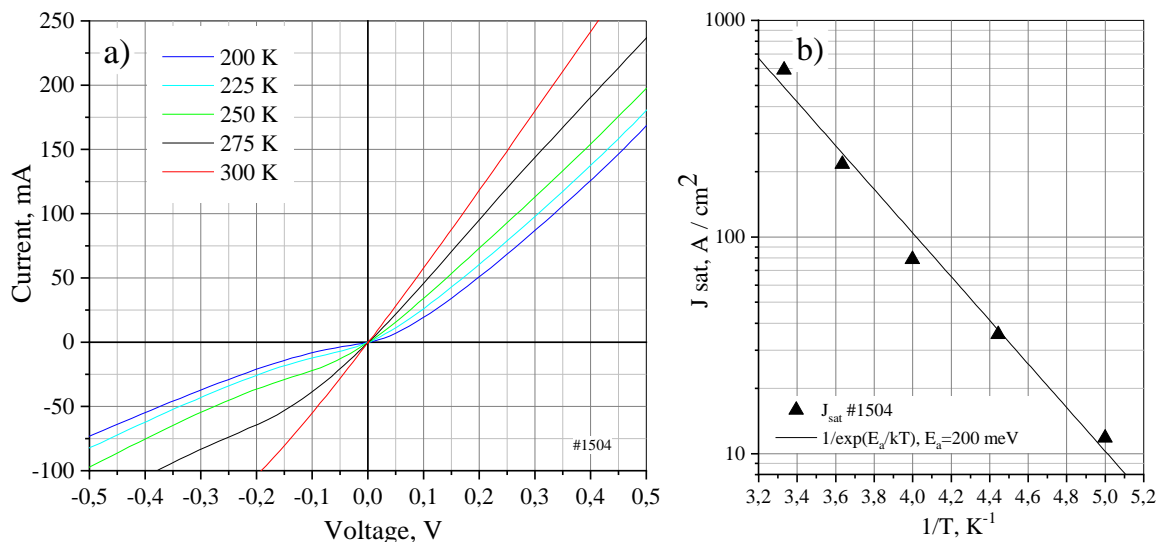


Figure 3 (a, b). (a) Current-voltage characteristics in 200 \div 300 K temperature range; (b) Temperature dependence of dark current.

In Figure 4 (a) shows the photosensitivity spectra of experimental samples of photodetectors with an immersion lens in the photovoltaic mode without external bias in the temperature range 80 \div 300 K.

The short-wavelength photoresponse cut-off at room temperature is located about 3.5 μm and is determined by absorption in an undoped n-InAs substrate. The long-wavelength boundary ranges from 9.0 to 9.5 μm . As can be seen from the graph, a decrease in temperature leads to: slight shift of the short-wavelength boundary of the photoresponse, which is associated with an increase in the band gap of the substrate; shift in the photosensitivity maximum and the long-wavelength boundary of the photoresponse, because of the increase of the photosensitive layer band gap; increase in the current sensitivity up to more than 1 A / W at 200 K, because of the increase of p-n junction resistance and the appearance of conditions for effective separation of carriers. With a further decrease in temperature ($T < 200$ K), the current sensitivity changes only slightly, which is apparently due to the fact that the quantum efficiency reaches a maximum for a given structure thickness.

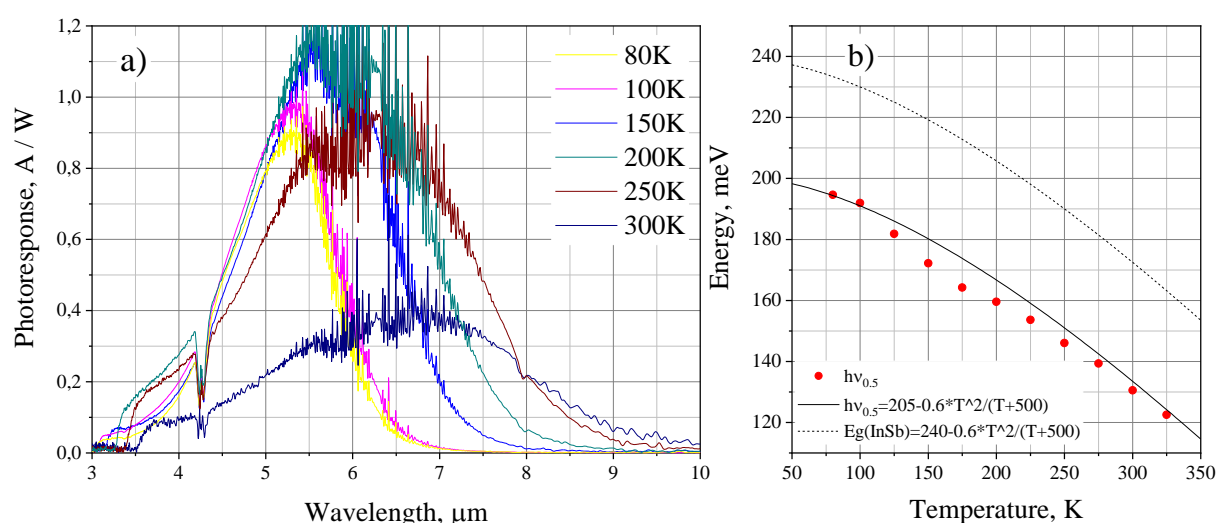


Figure 4(a, b). (a) Photoresponse at 80 ÷ 300 K temperature range; (b) Temperature dependences of the long-wavelength photosensitivity limit $h\nu_{0.5}$, InSb band gap and $h\nu_{0.5}$ approximation.

It is convenient to analyze the temperature dependences of the photosensitivity spectra by comparing them with the temperature dependence of the band gap of the nearest binary compound whose parameters are most fully studied. In Figure 4 (b) shows: the temperature dependence of the long-wavelength cut-off of the photosensitivity ($h\nu_{0.5}$), determined at a level of 0.5 on the maximum value at a given temperature, which usually corresponds to the band gap of the photosensitive region with accuracy to the energy of the impurity band, which in our case is about 10 meV and is assigned to the levels Zn [3]; bandgap InSb; approximation of $h\nu_{0.5}$ by a function with coefficients used to describe the temperature dependence of the band gap of InSb. As can be seen from the figure, under cooling, the behavior of the temperature dependence of the long-wavelength cut-off is well described by the function $h\nu_{0.5} f(T) = 205 - 0.6 \times T^2 / (T + 500)$ with coefficients corresponding to the temperature dependence of the band gap of InSb. The deviation appears in the temperature range $T > 250$ K, which may be associated with an increase in the contribution to absorption of a wider-gap layer of the photosensitive structure.

In Figure 5 shows the dependence of the dark current density vs. the long-wavelength cut-off, obtained from the data in Figure 3 and the data on photodetectors based on InAsSb solid solution [2]. As can be seen from the graph, in the experimental samples of photodetectors obtained during this

stage (#1504), the increase in the reverse current corresponds to the exponential dependence of the dark current on the long-wavelength cut-off of the photoresponse, which indicates that the diffusion mechanism of the flow current is dominated.

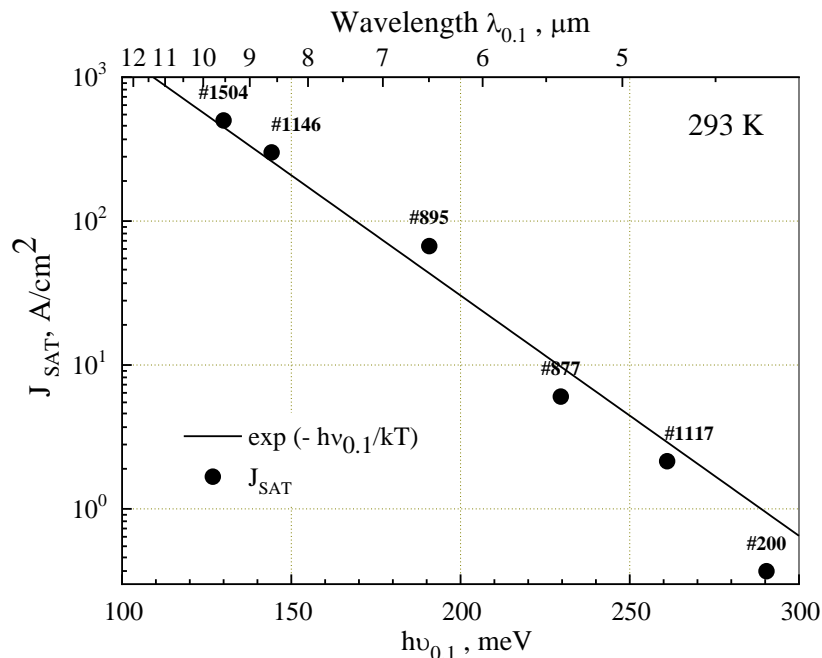


Figure 5. Dependence of the dark current density on the long-wavelength photosensitivity limit.

3. Conclusions

Experimental samples of photodetectors with a photosensitive region InAsSb_x ($0.3 < x < 0.35$) and a long-wavelength photosensitivity limit of about $9.5 \mu\text{m}$ have been tested and studied, including the measurement of current-voltage and spectral characteristics in a wide temperature range. It is shown that: in the temperature range of $200 \div 300 \text{ K}$, the p-n junction work is determined by the diffusion mechanism of current flow; current sensitivity values reach more than $1 \text{ A} / \text{W}$ at temperatures attainable with thermoelectric cooling; the temperature dependence of the long-wavelength edge is close to the temperature dependence of the band gap of the nearest binary compound InSb .

Acknowledgments

The authors wish to thank A.A. Lavrov, N.D. Il'inskaya, A.A. Usikova and S.A. Karandashev for their valuable contribution and the staff at the Center of Multi-User Facilities "Material Science and Diagnostics for Advanced Technologies" for performing SIMS microanalysis.

The work at IoffeLED Ltd. was supported by the Federal program "Development of Large-Sized Photosensitive Elements for the Spectral Ranges of $2.5\text{--}3.5$, $2.5\text{--}4.5$, and $2.5\text{--}5.5 \mu\text{m}$ Based on InAs Heterostructures and InAsSbP Solid Solutions" (contract code 14.576.21.0104, ID: RFMEFI57618X0104).

References

- [1] Rogalsky A, Kopytko M, Martyniok P 2017 Antimonide-based infrared detectors (Bellingham: SPIE press)
- [2] N.D. Il'inskaya, S.A. Karandashev, A.A.Lavrov, B.A. Matveev, M.A. Remennyi, N.M. Stus', A.A. Usikova 2018 Phys. Status Solidi A **215** 7
- [3] http://www.matprop.ru/InSb_bandstr#Temperature
- [4] Ponomarenko V P 2018 Quantum photosensory, (Moscow: Orion)